NJC

Accepted Manuscript

This article can be cited before page numbers have been issued, to do this please use: L. Liang, L. Nie, M. Jiang, F. Bie, L. Shao, C. Qi, X. Zhang and X. Liu, *New J. Chem.*, 2018, DOI: 10.1039/C8NJ02183J.

ROYAL SOCIETY OF CHEMISTRY

rsc.li/njc

View Article Online
DOI: 10.1039/C8NJ02183J

Palladium immobilized on *in situ* cross-linked chitosan superfine fibers for catalytic application in the aqueous medium

Lulu Liang,[a] Li Nie,[a] Minjuan Jiang,[a] Fusheng Bie,[b] Linjun Shao,[*, a] Chenze Qi,[a]

X. Man Zhang,[b] Xuejing Liu[*, b]

[a]*Zhejiang Key Laboratory of Alternative Technologies for Fine Chemicals Process, Shaoxing University, Zhejiang Province 312000, People's Republic of China, and* [b]*College of Chemistry, Chemical Engineering and Material Science, Zaozhuang University, Zaozhuang, Shandong, 277160, China*

*Address correspondence to Linjun Shao (shaolinjun@usx.edu.cn)

View Article Online
DOI: 10.1039/C8NJ02183J

Abstract

Chitosan composite superfine fibers with diameter of 321 ± 99 nm were prepared by electrospinning with PEO as the co-spinning polymer and itaconic acid as the *in situ* cross-linking agent. Itaconic acid was homogeneously dispersed in the chitosan fiber and the *in situ* cross-linking enabled the prepared chitosan composite fiber with improved solvent resistance, thermostability and mechanical strength. Palladium species immobilized on these annealed chitosan fibers can efficiently catalyze the reduction reaction of 4-nitrophenol as well as the Mizoroki-Heck reaction of aromatic iodides with *n*-butyl acrylates in aqueous medium. Furthermore, the larger fiber structure can facilitate the recovery and reuse of the palladium catalyst. The remarkable catalytic performance and easy recovery make this novel fiber supported palladium catalyst hold great potential applications in the green chemistry.

Keywords: Chitosan; Electrospinning; Cross-linking; Palladium; Heterogeneous

View Article Online
DOI: 10.1039/C8NJ02183J

Introduction

Chitosan, derived from deacetylation of biopolymer chitin, has excellent biocompatibility, biodegradability and adsorption properties, thus it holds great potential applications in medicine, food, chemistry and waste water treatment [1-3]. As chitosan contains abundant amine and hydroxyl groups, which could chelate with the active transition metal species, it has been fabricated into various shapes as excellent stabilizers and solid matrices to support the transition metal catalysts [4-7]. Recently, chitosan superfine fibers have attracted great interest as the solid matrices for immobilization of transition metal catalysts because of its easier recovery and larger specific surface area [8-10].

Electrospinning is a unique technique to fabricate the polymer solution or melt into fibers with diameter ranging from hundreds nanometer to several microns [11]. Trifluoroacetic acid (TFA) is often required as the solvent for chitosan to be processed by the electrospinning though it is expensive and toxic [12]. Blending chitosan with a second water soluble polymer (e.g. polyethylene oxide and polyvinyl alcohol) as the co-spinning agent is another effective way to prepare uniform chitosan fibers by electrospinning [13-15]. Moreover, a carefully selected polymer could even improve the physical and chemical properties of the composite fibers. Since chitosan fibers are unstable and easily soluble in the acidic solution, cross-linking is usually required by treatment with the cross-linking agent (e.g. glutaraldehyde and epichlorohydrin)

View Article Online
DOI: 10.1039/C8NJ02183J

[16-18]. However, the mechanical strength and chelating ability of chitosan fibers could be reduced after cross-linking with glutaraldehyde because glutaraldehyde was primarily reacted with the surface amine groups of chitosan fiber, whereas the fiber chitosan chains could not be homogeneously cross-linked [18].

In this study, the cross-linker itaconic acid was used to incorporate into the chitosan composite fibers. After electrospinning, *in situ* thermal cross-linking was induced to improve the solvent resistance, thermostability and mechanical strength for the composite fiber. Moreover, the cross-linked chitosan composite fibers could effectively chelate with the palladium species (Figure 1). This novel chitosan fiber supported palladium catalyst exhibites remarkable activity and stability to catalyze the reduction reaction of 4-nitrophenol as well as the Mizoroki-Heck reaction of aromatic iodides with olefins in aqueous medium.

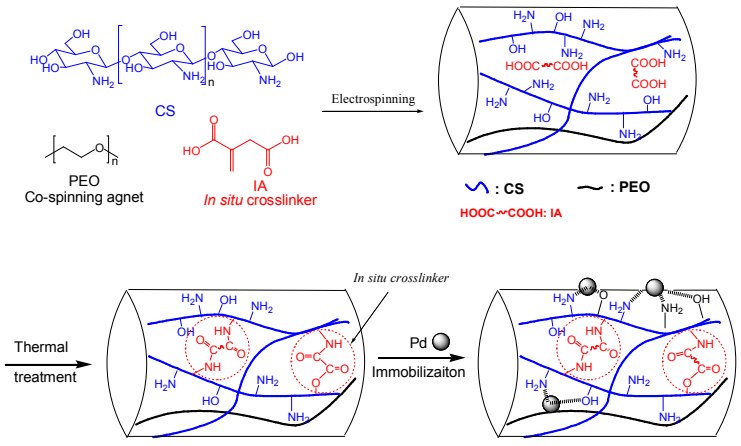

Figure 1. Schematic diagram for fabrication of the Pd-CS/PEO/IA fibers.

View Article Online
DOI: 10.1039/C8NJ02183J

Experimental

Materials

Chitosan (CS) (pharmaceutical grade, $M_n = 2.0 \times 10^4$, deacetylated degree: 95 %) was bought from Zhejiang Aoxing Biotechnology Co., Ltd (Zhejiang, China). $PdCl_2$ (chemical purity) was purchased from Hangzhou Changqing Chemical Industrial Co. Ltd (Zhejiang, China). Poly(ethylene oxide) (PEO) (average molecular weight = 1.0×10^6), itaconic acid (IA) (analytical grade), cetryltrimethyl ammonium bromide (CTAB) (analytical grade), tetrabutyl ammonium bromide (TBAB) (analytical grade) and PEG-2000 were bought from Aladdin Industrial Co. Ltd (Shanghai, China). Deionized water was used in all experiments.

Preparation of the cross-linked CS/PEO/IA composite fibers

Chitosan (0.95 g), PEO (0.05 g) and IA (0.20 g) were dissolved in 19 g 80% acetic acid aqueous solution and stirred overnight to achieve homogeneous solution. The solution was then applied into the electrospinning apparatus (FM1206, Beijing Future Material Sci-tech Co., Ltd, China) to prepare chitosan composite fibers. The optimized electrospinning parameters were: inner diameter of needle: 0.51 mm; feed rate: 1.2 mL/h; applied voltage: 18 kV; work distance: 15 cm. The resultant fiber mat was dried under vacuum to remove the residual solvent at 100 ^oC, followed by annealing at 150 ^oC for 12 hrs. The CS/PEO fibers were also prepared using the similar preparation protocol for the CS/PEO/IA composite fibers without addition of

View Article Online
DOI: 10.1039/C8NJ02183J

IA.

Immobilization of palladium on cross-linked CS/PEO/IA composite fibers

The CS/PEO/IA fiber mat (1.0 g) was added to a round-bottom flask containing 25 mg $PdCl_2$, 17 mg NaCl and 5 g H_2O (Na_2PdCl_4 aqueous solution), which was allowed to stir at 25 ^oC for 12 hrs, followed by addition of 0.5 g hydrazine (80%) to reduce the Pd^{2+} into Pd^0 species. After reduction, the fiber mat turned back, indicative of palladium immobilization on the fibers. The fibers supported palladium catalyst (Pd-CS/PEO/IA) was filtered, and then dried under a reduced pressure at 50 ^oC for 12 hrs.

The palladium content of the Pd-CS/PEO/IA catalyst was determined according to the following protocol: 20 mg Pd-CS/PEO/IA was completely decomposed in 5 mL mixture of fuming HNO_3 and H_2SO_4 (v/v: 1/1) at 80 ^oC, then diluted to 50 mL with deionized water. The palladium concentration was determined by means of inductively coupled plasma-atomic emission spectroscopy, which was allowed to calculate the palladium content (1.35%) for the Pd-CS/PEO/IA catalyst.

Reduction of 4-nitrophenol catalyzed by the fiber catalyst

Fresh prepared $NaBH_4$ aqueous solution (2.0 mL, $NaBH_4$ content: 0.65 mmol), 4-nitrophenol aqueous solution (2.0 mL, *p*-nitrophenol content: 6.5 μmol) and 46 mL water were added into a 100 mL flask, followed by addition of the Pd-CS/PEO/IA (5.0 mg, Pd: 0.63 μmol), then stirred vigorously to reduce the diffusion influence at room

View Article Online
DOI: 10.1039/C8NJ02183J

temperature. The reductive reaction was monitored by UV-Vis analysis. After completion, the Pd-CS/PEO/IA catalyst was recovered by filtration and washed with water and ethanol. The recovered catalyst was dried under reduced pressure at 50 ^{o}C for 12 hrs.

General procedure for the Mizoroki-Heck reaction catalyzed by the fiber catalyst

Aromatic iodides (0.7 mmol), olefins (1.4 mmol), Pd-CS/PEO/IA (50 mg, Pd: 6.3 μmol), CTAB (63 μmol) and CH_3COOK (2.1 mmol) and deionized water (5.0 g) was added to a 20 mL tubular reactor equipped with a magnetic stir bar. The mixture was allowed to stir at 100 ^{o}C for 24 hrs. The reaction was extracted with ethyl acetate for three times (3 × 20 mL). The combined organic layer was washed with water, and then dried over anhydrous Na_2SO_4, and the solvent was removed under reduce pressure. The coupling products were obtained by purification using silica gel chromatography with a mixture of petroleum ether and ethyl acetate (v/v: 8/1), and the chemical structures were confirmed by ^{1}H NMR spectroscopy. The Pd-CS/PEO/IA catalyst was filtered from the mixture, then washed with *N*,*N*–dimethylformamide, water and ethanol. The recovered Pd-CS/PEO/IA catalyst was dried under reduced pressure at 50 ^{o}C for 12 hrs.

Characterization

The morphologies of the fiber mats were observed with a scanning electron microscope (SEM) (Jeol, Jsm-6360lv, Japan). The SEM samples were coated with a

View Article Online
DOI: 10.1039/C8NJ02183J

2-3 nm layer of Pt to make them conductive. The fiber diameters were acquired from the SEM images. The elemental analysis was determined by means of an energy dispersive X-ray spectroscopy (Oxford EDX System). The chemical structures of fiber mats were analyzed by Fourier transform infrared spectroscopy (FT-IR) with the accessories of attenuated total reflection (Nicolet, Nexus-470, USA). The thermostability of the fiber mat was analyzed using a thermogravimetric analyzer (TGA) (Beijing Scientific Instrument Factory, China) in air. The heating ramp was set from 40 to 550 ^{o}C at a rate of 20 ^{o}C/min. UV-Vis absorption spectrum was recorded on a UV-1800PC spectrometer (Mapada, China). The quantitative analysis of Mizoroki-Heck reaction products was carried out via Agilent GC/MS (Agilent, GC6890/5975 MSD, USA). The dispersion of palladium nanoparticles in the Pd-CS/PEO/IA was analyzed by X-ray diffraction (XRD) (Empyrean, PANalytical, Netherlands). ^{1}H NMR spectra were recorded in $CDCl_3$ (Bruker, AVANCE III 400 MHz, Switzerland) and the proton chemical shifts are reported in ppm relative to TMS as the internal reference. Multiplicities are reported as: singlet (s), doublet (d), and multiplet (m). Inductively coupled plasma-atomic emission spectroscopy (ICP-AES) analysis was performed on a Leemann ICP-AES Prodigy XP (Leeman Labs, USA). The mechanical analysis was carried out on the electronic fabric strength tester (YG065HC/PC, Shandong Lanzhou Electron Instrument Co., Ltd, China). The specific surface area of the CS/PEO/IA fiber mat was determined by the standard Brunaver-Emmett-Teller (BET) method on the specific surface area and porosity

View Article Online
DOI: 10.1039/C8NJ02183J

analyzer (Empyrean, Micromeritics, USA). X-ray photoelectron spectroscopic (XPS) was performed by angle-resolved photoemission spectroscopy (ADES-400, VG Co. UK). C_{1s} of 284.6 eV was used as the internal reference for calibration.

Results and Discussion

Characterization of the Pd-CS/PEO/IA catalyst

Blending chitosan with PEO for electrospinning is a unique efficient technique to prepare continuous chitosan superfine fibers [12,13,17,21]. The CS/PEO fibers with diameter of 321 ± 99 nm were successfully prepared with merely 5% of PEO-loading (Figure 1A). Although the CS/PEO fiber mat was annealed at 150 ^{o}C for 12 hrs, the fiber structure was found to be completely damaged after submersing in 50 wt.% acetic acid solution for 24 hrs (Figure 2B). The CS/PEO/IA fiber mats with 10%, 20% and 30% loadings of IA were also prepared to examine their solvent resistance (Figure 2C and S1). Figure 2D and S1 shows that the CS/PEO/IA fibers with 10% loading of IA has been seriously swollen, whereas the fibers with 20% and 30% loadings of IA are well retained after submersing in 50 wt.% acetic acid solution for 24 hrs. Thus, 20% loading of IA was chose to crosslink the CS/PEO/IA fibers for this study.

View Article Online
DOI: 10.1039/C8NJ02183J

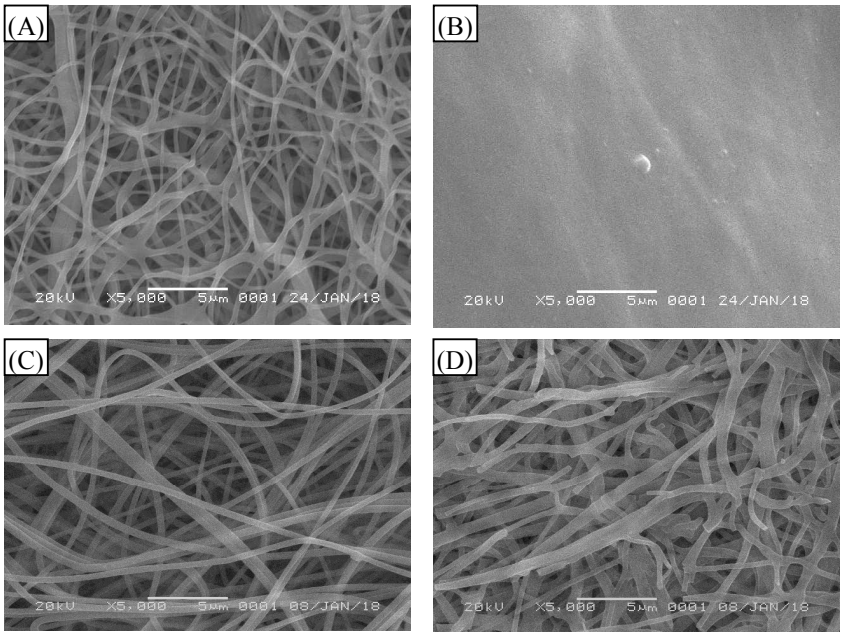

Figure 2. SEM images of the CS/PEO fiber mat (A, B) and the CS/PEO/IA fiber mat with 20 wt.% of IA loading (C, D) before and after submersing in 50 wt.% acetic acid solution for 24 hrs.

The chemical structures of chitosan composite fiber mats were analyzed by FT-IR spectra (Figure 3). Compared with the FT-IR spectrum of the CS/PEO fiber mat, incorporation of IA into the fiber resulted in observation of a new absorption peak at 1706 cm^{-1} (>C=O of carboxyl group) for the CS/PEO/IA fiber mat. After annealing treatment, the absorption at 1706 cm^{-1} disappeared and a new band appeared at 1306 cm^{-1} (amide III), accompanied by intensifying absorption peak at 1653 cm^{-1} (amide I) [22]. These results indicate that the CS/PEO/IA fibers have been cross-linked by reactions of the carboxyl groups on IA with the amino groups of the chitosan to form the amide functional groups. After immobilization of the palladium species, the

View Article Online
DOI: 10.1039/C8NJ02183J

absorption peaks at 1563 cm^{-1} ($-NH_2$) and 1653 cm^{-1} (>C=O) are shifted, suggesting coordination of the fiber surface chitosan with the palladium species, thus the cross-linked CS/PEO/IA can effectively chelate with the palladium species.

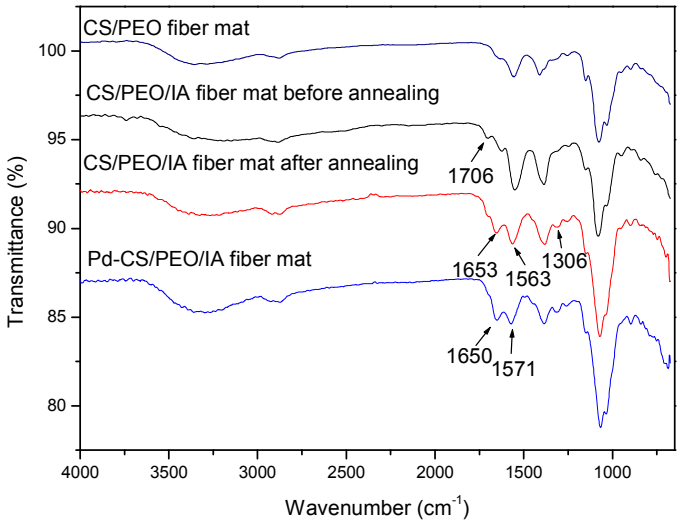

Figure 3. FT-IR spectra for the CS/PEO fiber mat and the CS/PEO/IA fiber mat before and after annealing treatment, together with the Pd-CS/PEO/IA fiber mat.

As the heterogeneous palladium catalysts are often used at relatively high reaction temperature, the thermostabilities of supporting materials are critical for their practical applications. Figure 4 shows that weigh loss of the CS/PEO/IA fiber mats before and after annealing treatment took place in three major stages. The first stage at 50-130 ^{o}C was assigned to loss of the adsorbed water. The predominant weight losses of the second (175-375 ^{o}C) and third stages (450-550 ^{o}C) may be attributed to the thermal oxidation, and carbonization of chitosan and PEO. The thermostability of the CS/PEO/IA fiber mat has been improved after annealing treatment. Moreover, tensile

View Article Online
DOI: 10.1039/C8NJ02183J

strength test shows that the tensile strength of the CS/PEO/IA fiber mat also increases from 4.30 MPa to 5.21 MPa after annealing treatment. The high tensile strength of the fiber mat could improve the resistance from damage in the following harsh reaction conditions. The BET surface was determined to be 9.53 m^2/g for the CS/PEO/IA fiber mat. The strong chelating ability, larger specific surface area, excellent mechanical strength and solvent resistance make this novel CS/PEO/IA fiber mat an ideal polymer matrix to support transition metal catalyst.

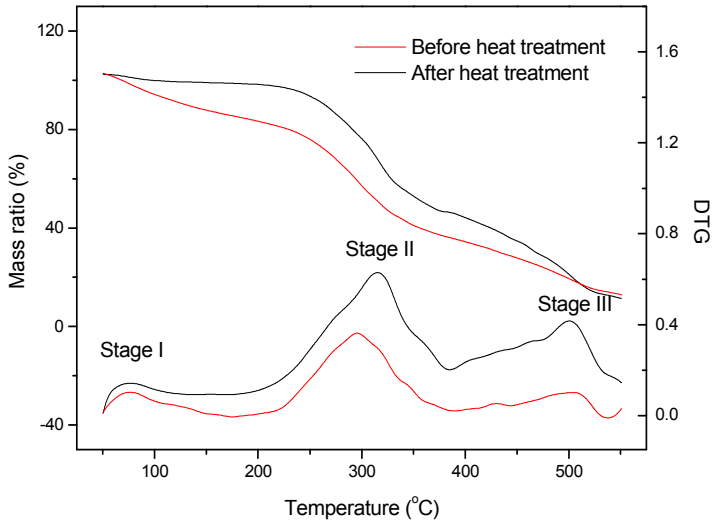

Figure 4. Thermal analysis results of CS/PEO/IA fiber mat before and after annealing treatment.

SEM-EDX characterization shows that the palladium species has been deposited homogeneously on the Pd-CS/PEO/IA fiber mat (Figure 5). Besides SEM-EDX characterization, the Pd-CS/PEO/IA was further analyzed by XRD (Figure 6). As chitosan is a partially crystalline polysaccharide due to its regular chain, it has a

View Article Online
DOI: 10.1039/C8NJ02183J

strong reflection peak at 18.4° [20,22]. The reflection peaks at 39.6°, 45.9° and 67.5° are associated with the (111), (200) and (220) planes of the face centered cubic (FCC) palladium particles [23-25]. Based on the Scherrer equation [24,25], the reflection peaks suggest an average size of palladium particles (*d*) closed to 9.3 nm. XPS analysis shows that the palladium $3d_{5/2}$ and $3d_{3/2}$ electron binding energies of the Pd-CS/PEO/IA catalyst are about 1.3 eV lower after than before reduction, indicating the reduction of the divalent Pd^{2+} into the Pd^{0} species (Figure S2).

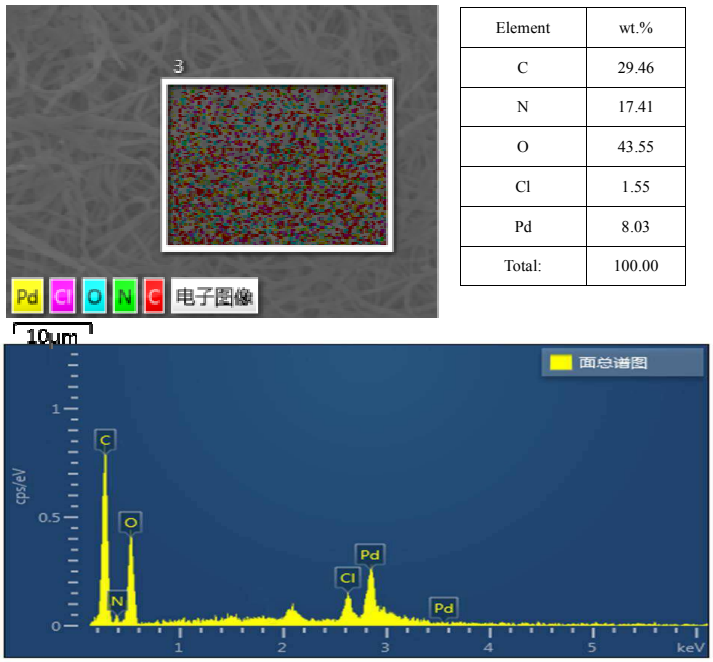

Element	wt.%
C	29.46
N	17.41
O	43.55
Cl	1.55
Pd	8.03
Total:	100.00

Figure 5. SEM-EDX analysis of the Pd-CS/PEO/IA.

View Article Online
DOI: 10.1039/C8NJ02183J

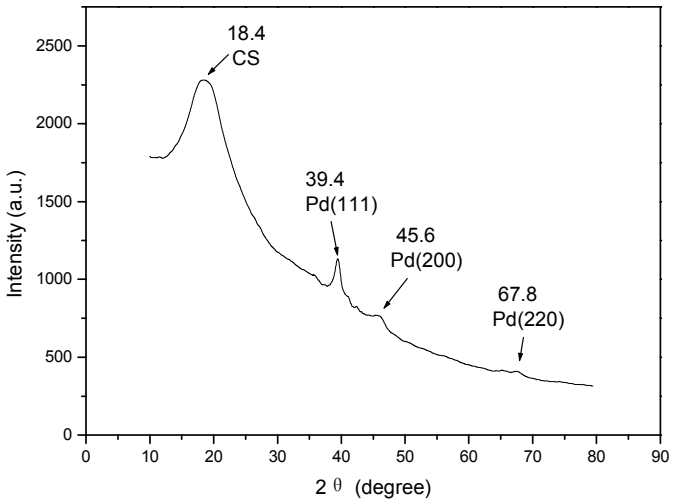

Figure 6. XRD pattern of the Pd-CS/PEO/IA.

Reduction of 4-nitrophenol catalyzed by the Pd-CS/PEO/IA catalyst

Since nitrophenols and their derivatives are highly toxic pollutants derived from pesticides, herbicides, insecticides and synthetic dyes, it is important to reduce them into much less toxic aminophenols [5,26,27]. The catalytic activity of the Pd-CS/PEO/IA catalyst has been investigated for the reductive reaction of 4-nitrophenol with excess $NaBH_4$ in aqueous medium. The reductive reaction is very slow without addition of the palladium catalyst (Figure 7), but the 4-nitrophenol conversion can reach nearly 100 % within 30 min when catalyzed with the Pd-CS/PEO/IA.

View Article Online
DOI: 10.1039/C8NJ02183J

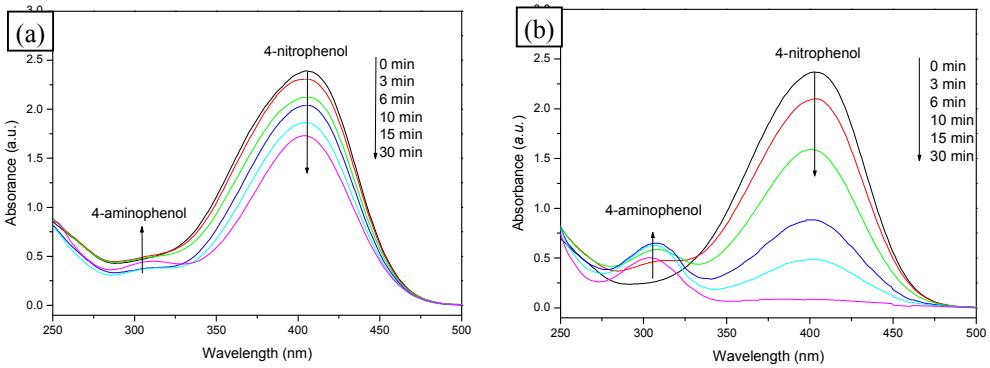

Figure 7. UV-Vis spectra for the reductive reactions of 4-nitrophenol: (a) no catalyst and (b) with the Pd-CS/PEO/IA. Reaction condition: 0.65 mmol $NaBH_4$, 6.5 μmol 4-nitrophenol and 0.63 μmol Pd-CS/PEO/IA in 50 mL water at 25 ^oC for 30 min.

The reductive reaction of 4-nitrophenol into 4-aminophenol was believed to proceed via the pseudo-first-order kinetics in excess of $NaBH_4$ when catalyzed by metal catalysts [27]. The reaction was examined using the pseudo-first-order kinetic model according to the following kinetic equation (Eq 1).

$$\ln (C_t/C_0) = \ln (A_t/A_0) = -k_{app}t \qquad (1)$$

where C_0 and C_t are the 4-nitrophenol concentrations at initial time and time t, respectively. The concentration ratio C_t/C_0 can be determined from the absorbance ratio of 4-nitrophenol A_t (at time t) to A_0 (at initial time). As shown in Figure 8, the apparent rate constant (k_{app}) were obtained to be 1.76×10^{-4} s^{-1} and 1.91×10^{-3} s^{-1} for no catalyst and with the Pd-CS/PEO/IA, respectively. Interestingly, the rate constant for the Pd-CS/PEO/IA is comparable with the literature results [27,28].

View Article Online
DOI: 10.1039/C8NJ02183J

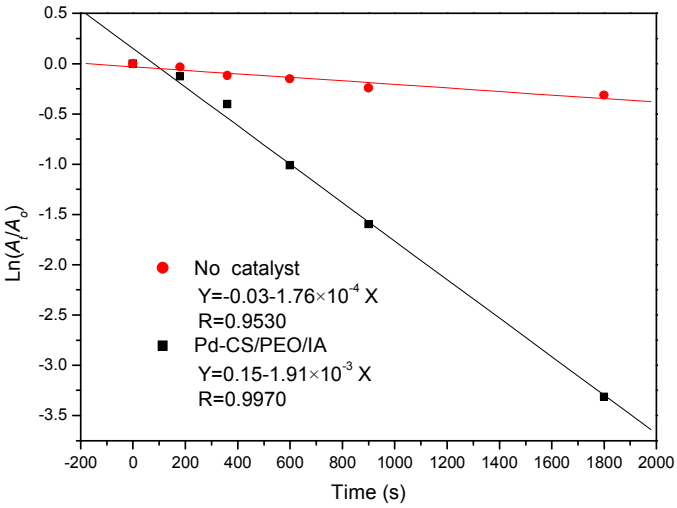

Figure 8. Plot of $\ln(A_t/A_0)$ verses reaction time for the reductive reaction of 4-nitrophenol by no catalyst and the Pd-CS/PEO/IA catalyst.

The heterogeneous catalysts have advantage for their relatively easy separation and reuse of the expensive transition metals. Generally, supporting materials are prepared into small fine particles to maximize the surface area to enhance the catalytic activities. Compared to the tiny particles, the larger fiber structure ensures the easy separation of the Pd-CS/PEO/IA catalyst from the reaction mixture. As shown in Figure 9, the Pd-CS/PEO/IA catalyst can be reused for 5 times without obvious loss of activity.

View Article Online
DOI: 10.1039/C8NJ02183J

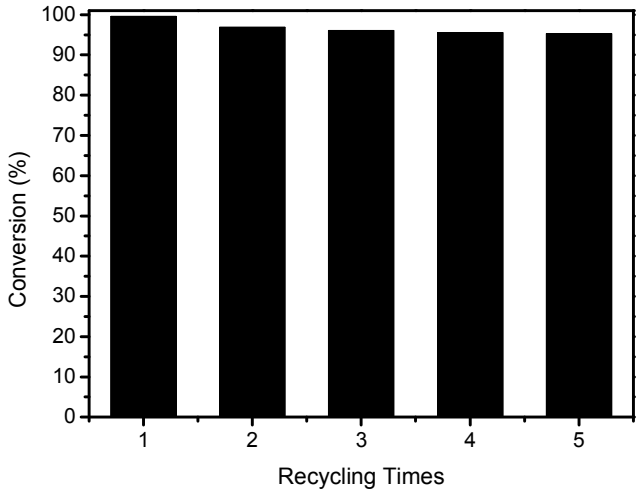

Figure 9. Dependence of the 4-nitrophenol conversion with the recycling times for the Pd-CS/PEO/IA. Reaction condition: 0.65 mmol $NaBH_4$, 6.5 μmol 4-nitrophenol and 0.63 μmol Pd-CS/PEO/IA in 50 mL water at 25 ^oC for 30 min.

Mizoroki-Heck reaction catalyzed by the Pd-CS/PEO/IA

Mizoroki-Heck reaction was one of the most powerful and straightforward methods for construction of the sp^2-sp^2 carbon-carbon bonds [29,30], which attracts the interests to search for more environmental benign reaction conditions [31,32]. Heterogeneous palladium catalyst has also attracted much attention for their easy recovery and reuse of expensive and toxic palladium catalyst [33-35]. Furthermore, different green solvents have been evaluated for this reactions [36-38]. Among the various solvent, water is clearly the ideal green solvent. In order to improve the solubility of organic substrates in water, a phase transfer agent (PTA) is generally needed to promote the reaction. The quaternary ammonium salt can stabilize the

View Article Online
DOI: 10.1039/C8NJ02183J

zero-valent palladium species, and the long alkyl chain can also increase the dispersion of reaction substrates [39,40]. Examination of entries 1-4 in Table 2 shows that CTAB is the most effective PTA to promote the reaction, and the Mizoroki-Heck reaction yield increases with the CTAB loading (Entry 4-6 in Table 1). The optimal *n*-butyl cinnamate yield (89%) can be obtained when the CTAB/Pd ratio reaches 10, and no further improvement of the reaction yields has been observed with higher CTAB/Pd ratios.

Table 1. Effect of phase transfer reagent on the Pd-CS/PEO/IA catalyzed Mizoroki-Heck reactions of iodobenzene with methyl acrylate [a]

Entry	PTA	PTA/Pd ratio	Conversion[b] (%)	Yield[b] (%, *trans*)
1	No	0	21	17
2	PEG-2000	1	25	22
3	TBAB	1	30	27
4	CTAB	1	70	61
5	CTAB	5	89	76
6	CTAB	10	96	89
7	CTAB	15	98	90

[a] Reaction conditions: 0.7 mmol iodobenzene, 1.4 mmol methyl acrylate, 2.1 mmol potassium acetate, 6.3 μmol Pd-CS/PEO/IA, and PTA in 5.0 g water at 100 ^{o}C for 24

View Article Online
DOI: 10.1039/C8NJ02183J

hrs.

[b] GC-MS conversion and yield based on the amount of iodobenzene.

Mizoroki-Heck reactions require suitable bases to neutralize the acidic byproducts, otherwise they would be suppressed. Examination of entry 1 in Table 2 shows that the coupling yield of methyl cinnamate is only 27% without base. Entries 3-6 in Table 2 shows that the potassium compounds are more effective than the sodium compounds, whereas carbonate is more effective than hydroxide at promoting the Pd-CS/PEO/IA catalyzed Mizoroki-Heck reaction. Triethylamine has comparable activity with K_2CO_3 as base (Entry 7 in Table 2). Among the tested bases, potassium acetate is the most effective base to promote the Pd-CS/PEO/IA catalyzed Mizoroki-Heck reaction with yield of 89% (Entry 2 in Table 2). Thus, potassium acetate has been chosen for the following experiments.

Table 2. Base effects on the Pd-CS/PEO/IA catalyzed Mizoroki-Heck reactions of iodobenzene with methyl acrylate.[a]

Entry	Base	Conversion[b] (%)	Yield[b] (%)
1	No	29	27
2	KOAc	96	89
3	KOH	70	54
4	K_2CO_3	75	71
5	NaOH	32	32

View Article Online
DOI: 10.1039/C8NJ02183J

6	Na_2CO_3	67	66
7	Et_3N	81	67

[a]Reaction conditions: 0.7 mmol iodobenzene, 1.4 mmol methyl acrylate, 2.1 mmol base, 6.3 μmol Pd-CS/PEO/IA, and 63 μmol PTA in 5.0 g water at 100 ^oC for 24 hrs. [b]GC-MS conversion and yield based on the amount of iodobenzene.

Table 3 shows that high temperature is beneficial for both iodobenzene conversion and methyl cinnamate yield. No coupling product was detected when the reaction was carried out below 80 ^oC, whereas iodobenzene was almost consumed for the reaction with methyl acrylate at 100 ^oC. Thus, the optimal reaction temperature is 100 ^oC for the Pd-CS/PEO/IA catalyzed Mizoroki-Heck reaction.

Table 3. Temperature effects on the Pd-CS/PEO/IA catalyzed Mizoroki-Heck reactions of iodobenzene with methyl acrylate.[a]

Entry	Temperature (^oC)	Conversion[b] (%)	Yield[b] (%)
1	80	~0	~0
2	90	55	46
3	95	86	83
4	100	96	89

[a]Reaction conditions: 0.7 mmol iodobenzene, 1.4 mmol methyl acrylate, 2.1 mmol base, 6.3 μmol Pd-CS/PEO/IA, and 63 μmol PTA in 5.0 g water for 24 hrs.

View Article Online
DOI: 10.1039/C8NJ02183J

[b]GC-MS conversion and yield based on the amount of iodobenzene.

The Pd-CS/PEO/IA catalyst is also effective for the Mizoroki-Heck reactions of other aryl iodides with olefins, as evident in Table 4. Entries 2-5 in Table 4 shows that the Pd-CS/PEO/IA catalytic system is tolerant for both electron-rich and electron-deficient aromatic iodides to produce the corresponding reaction products in excellent yields. The relatively low coupling yield of 1-iodo-2-methylbenzene with *n*-butyl acrylate could be attributed to the steric hindrance of 2-methyl group (Entry 6 in Table 4). The Pd-CS/PEO/IA catalyst also exhibits high activity for the mono-substituted acrylates (Entries 7 and 8 in Table 4).

Table 4. Pd-CS/PEO/IA catalyzed Mizoroki-Heck reactions of various aromatic halides with different olefins in the aqueous medium.[a]

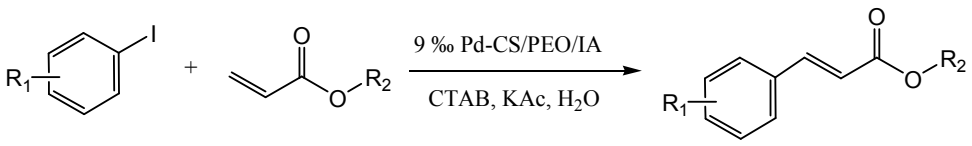

Entry	Aromatic iodides	Olefin	Conversion (%)	Yield (%, *trans*)
1	PhI	*n*-butyl acrylate	95	89
2	4-FPhI	*n*-butyl acrylate	95	87
3	4-BrPhI	*n*-butyl acrylate	99	91
4	4-ClPhI	*n*-butyl acrylate	98	90

View Article Online
DOI: 10.1039/C8NJ02183J

5	4-CH_3PhI	*n*-butyl acrylate	99	97
6	2-CH_3PhI	*n*-butyl acrylate	96	87
7	PhI	methyl acrylate	96	89
8	PhI	CH_2=CH-Ph	88	81

[a] Reaction conditions: 0.7 mmol aromatic iodides, 1.4 mmol olefin, 2.1 mmol potassium acetate, 6.3 μmol Pd-CS/PEO/IA, and 63 μmol CTAB in 5.0 g water at 100 ^{o}C for 24 hrs.

[b] GC-MS conversion and yield based on the amount of aromatic halides.

The reusability of Pd-CS/PEO/IA for the Mizoroki-Heck reaction has been examined, and the results have been summarized in Figure 10. The catalytic activities of the recovered Pd-CS/PEO/IA catalyst retain over five cycles for the Mizoroki-Heck reaction of iodobenzene with *n*-butyl acrylate. Moreover, the fiber structure of the recovered Pd-CS/PEO/IA catalyst is still well retained (Figure S3). The palladium content (0.83%) in the recovered Pd-CS/PEO/IA catalyst indicates that only about 26% of the immobilized palladium species had been leached after 5 cycles of applications. The remarkable stability of the Pd-CS/PEO/IA catalyst can be associated with the strong chelation of the palladium species with the amine groups on the fiber surface.

View Article Online
DOI: 10.1039/C8NJ02183J

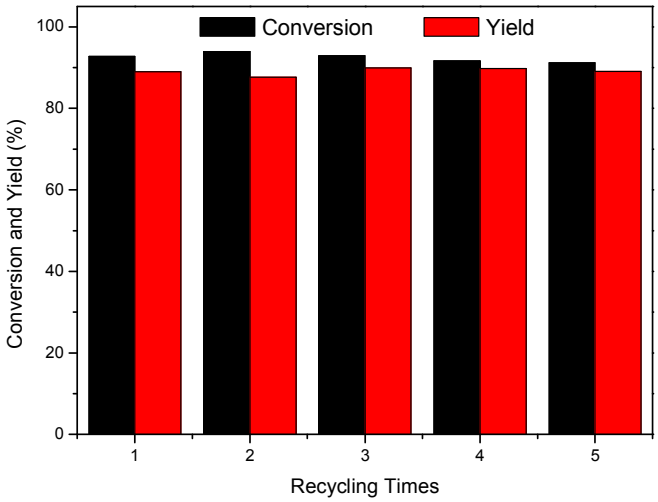

Figure 10. Dependence of the Mizoroki-Heck reaction conversions and yields with the recycling times for the Pd-CS/PEO/IA catalyst. Reaction condition: 0.7 mmol iodobenzene, 1.4 mmol *n*-butyl acrylate, 2.1 mmol potassium acetate, 6.3 μmol Pd-CS/PEO/IA, and 63 μmol CTAB in 5.0 g water at 100 ^{o}C for 24 hrs.

Conclusions

In summary, we have demonstrated a facile approach to fabricate the cross-linked chitosan superfine fibers. *In situ* cross-linking was induced in the fiber to enhance its solvent resistance, thermostability and mechanical strength. This cross-linked chitosan fiber holds great potential as the supporting material to chelate the palladium catalyst, larger surface area of superfine fiber structure, and stability in aqueous medium. As a demonstration, palladium catalyst has been immobilized on these crosslinked CS/PEO/IA superfine fibers, which was shown as an efficient and stable

View Article Online
DOI: 10.1039/C8NJ02183J

heterogeneous palladium catalyst for the reductive reaction of 4-nitrophenol as well as the Mizoroki-Heck reactions of aromatic iodides with olefins in the aqueous medium.

Acknowledgement

The authors thanks very much for the financial support from the National Natural Science Foundation of China (Grant No. 11705117).

Reference

1 J. Desbrières and E. Guibal, *Polym. Int.*, 2018, 67, 7.

2 A. Ali and S. Ahmed. *Int. J. Biol. Macromol.,* 2018, 109, 273.

3 H. Wang, J. Qian and F. Ding. *J. Agric. Food Chem.*, 2017, 66, 395.

4 N. B. Yılmaz, T. Baran and A. Menteş. *Carbohyd. Polym.*, 2018, 181, 596.

5 C. Zhang, D. Lu, P. Jiang, J. Li and Y. Leng. *Catal. Lett.,* 2017*,*147, 2534.

6 Anuradha, S. Kumari, S. Layek and D. D. Pathak. *New J. Chem.*, 2017, 41, 5595.

7 M. Lee, B. Y. Chen and W. Den. *Appl. Sci.*, 2015, 5, 1272.

8 S. S. Shen, J. J. Yang, C. X. Liu and R. B. Bai. *RSC Adv.*, 2017, 7, 10424.

9 S. Lin, W. Wei, X. Wu, T. Zhou, T. Mao and Y. S. Yun. *J. Hazard. Mater.*, 2015, 299, 10.

10 W. Tighzert, A. Habi, A. Ajji, T. Sadoun and B. O. Daoud. *Fiber. Polym.*, 2017, 18,

View Article Online
DOI: 10.1039/C8NJ02183J

514.

11 F. E. Ahmed, B. S. Lalia and R. Hashaikeh. *Desalination*, 2015, 356, 15.

12 K. Sun and Z. H. Li. *Express Polym. Lett.*, 2011, 5, 342.

13 K. A. Rieger, N. P. Birch and J. D. Schiffman. *Carbohyd. Polym.*, 2016, 139, 131.

14 M. Koosha, H. Mirzadeh, M. Shokrgozar and M. Farokhi. *RSC Adv.*, 2015, 5, 10479.

15 W. Zhang, L. Zhao, J. Ma, X. Wang, Y. Wang, F. Ran, H. Ma and S. Yu. *Fiber. Polym.*, 2017, 18, 922.

16 S. R. Gomes, G. Rodrigues, G. G. Martins, M. A. Roberto, M. Mafra, C. M. R. Henriqures and J. C. Silva, *Mater. Sci. Eng. C-Mater. Biol. Appl.*, 2015, 46, 348.

17 J. L. Vondran, W. Sun and C. L. Schauer, *J. Appl. Polym. Sci.*, 2008, 109, 968.

18 Z. Wang, M. Xu, L. Shao and C. Qi, *Kinet. Catal.*, 2016, 57, 354.

19 C. K. S. Pillai, W. Paul and C. P. Sharma, *Prog. Polym. Sci.*, 2009, 34, 641.

20 L. Shao, Y. Ren, Z. Wang and C. Qi, Y. Lin, *Polymer*, 2015, 75, 168.

21 S. L. Mengistu, F. Bossard and M. Rinaudo, *Int. J. Mol. Sci.* 2016, 17, 1790.

22 I. Leceta, P. Guerrero, I. Ibarburu, M. T. Dueñas and K. D. L. Caba, *J. Food Eng.,* 2013, 116, 889.

23 S. Banerjee, K. Dasgupta, A. Kumar, P. Ruz, B. Vishwanadh, J. B. Joshi and V. Sudarsan, *Int. J. Hydrogen Energ.*, 2015, 40, 3268.

24 Q. Wang, Y. Wang, P. Guo, Q. Li, R. Ding, B. Wang, H. Li, J. Liu and X. S. Zhao, *Langmuir*, 2014, 30, 440.

View Article Online
DOI: 10.1039/C8NJ02183J

25 C. C. Li, R.Sato, M. Kanehara, H. B. Zeng, Y. Bando and T. Teranishi, *Angew. Chem. Int. Ed.*, 2009, 48, 6883.

26 S. M. El-Sheikh, A. A. Ismail and J. F. Al-Sharab, *New J. Chem.*, 2013, 37, 2399.

27 B. Naik and N. N. Ghosh. *Powder Technol.*, 2012, 232, 1.

28 K. L. Wu, X. W. Wei, X. M. Zhou, D. H. Wu, X.W. Liu, Y. Ye and Q. Wang, *J. Phys. Chem. C*, 2011, 115, 16268.

29 S. Layek, Anuradha, B. Agrahari and D. D. Pathak, *J. Organomet. Chem.*, 2017, 846, 105.

30 B. Agrahari, S. Layek, Anuradha, R. Ganguly and D. D. Pathak, *Inorg. Chim. Acta*, 2018, 471, 345.

31 F. Christoffel and T. R. Ward, *Catal. Lett.*, 2017, 2017, 1.

32 B. Movassagh and N. Rezaei, *New J. Chem.*, 2015, 39, 7988.

33 M. Azaroon and A. R. Kiasat, *Appl. Organomet. Chem.*, 2018, 32, e4271.

34 S. F. Motevalizadeh, M. Alipour, F. Ashori, A. Samzadeh-Kermani, H. Hamadi, M.R. GFanjali, H. Aghahosseini, A. Ramazani, M. Khoobi and E. Gholibegloo. *Appl. Organomet. Chem.* 2018, 32, e4123.

35 H. Veisi and N. Mirzaee. *Appl. Organomet. Chem.* 2018, 32, e4067.

36 M. Zarghani and B. Akhlaghinia. *B. Chem. Soc. Jpn.*, 2016, 89, 1192.

37 S. N. Jadhav and C. V. Rode, *Green Chem.*, 2017, 19, 5958.

38 D. Roy and Y. Uozumi, *Adv. Syn. Catal.*, 2018, 360, 602.

39 T. Jeffery, *Tetrahedron*, 1996, 52, 10113.

View Article Online
DOI: 10.1039/C8NJ02183J

40 M. H. Entezari and A. Keshavarzi, *Ultrason. Sonochem.,* 2001, 8, 213.

View Article Online
DOI: 10.1039/C8NJ02183J

Graphical Abstract